

FJSRL-TR-89-0002

FRANK J. SEILER RESEARCH LABORATORY

THRUST GENERATION BY AN
AIRFOIL IN HOVERING MODE

JANUARY 1989

DTIC
ELECTE
S 7 FEB 1989 D
E

PETER FREYMUTH

APPROVED FOR PUBLIC RELEASE:
DISTRIBUTION UNLIMITED.

2307-F1-38

AIR FORCE SYSTEMS COMMAND
UNITED STATES AIR FORCE

AD-A203785



90 9 7 006

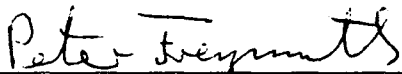
This document was prepared by the Aerospace Mechanics Division, Directorate of Lasers and Aerospace Mechanics, Frank J. Seiler Research Laboratory, United States Air Force Academy, CO. The research was conducted under Project Work Unit Number 2307-F1-38, Dr. Peter Freymuth was the Project Scientist in charge of the work.

When U.S. Government drawings, specifications or other data are used for any purpose other than a definitely related government procurement operation, the government thereby incurs no responsibility nor any obligation whatsoever, and the fact that the government may have formulated, furnished or in any way supplied the said drawings, specifications or other data is not to be regarded by implication or otherwise, as in any manner licensing the holder or any other person or corporation or conveying any rights or permission to manufacture, use or sell any patented invention that may in any way be related thereto.

Inquiries concerning the technical content of this document should be addressed to the Frank J. Seiler Research Laboratory (AFSC), FJSRL/NH, USAF Academy, CO 80840-6528. Phone (719) 472-3122.

[This report has been reviewed by the Commander and is releasable to the National Technical Information Service (NTIS). At NTIS it will be available to the general public, including foreign nations.]

This technical report has been reviewed and is approved for publication.


PETER FREYMUTH
Visiting Research Professor


ROBERT F. REILMAN, JR., Major, USAF
Director, Lasers & Aerospace Mechanics


WILLIAM G. THORPE, Lt Col, USAF
Commander

Copies of this report should not be returned unless return is required by security considerations, contractual obligations, or notice on a specific document.

Printed in the United States of America. Qualified requestors may obtain additional copies from the Defense Documentation Center. [All others should apply to: National Technical Information Service, 6285 Port Royal Road, Springfield, Virginia 22161.]

REPORT DOCUMENTATION PAGE

1a. REPORT SECURITY CLASSIFICATION Unclassified			1b. RESTRICTIVE MARKINGS			
2a. SECURITY CLASSIFICATION AUTHORITY			3. DISTRIBUTION/AVAILABILITY OF REPORT			
2b. DECLASSIFICATION/DOWNGRADING SCHEDULE						
4. PERFORMING ORGANIZATION REPORT NUMBER(S) FJSRL-TR-89-0002			5. MONITORING ORGANIZATION REPORT NUMBER(S)			
6a. NAME OF PERFORMING ORGANIZATION Frank J. Seiler Research Lab		6b. OFFICE SYMBOL (If applicable) FJSRL/NHM	7a. NAME OF MONITORING ORGANIZATION			
6c. ADDRESS (City, State and ZIP Code) USAF Academy Colorado Springs, CO 80840-6528			7b. ADDRESS (City, State and ZIP Code)			
8a. NAME OF FUNDING/SPONSORING ORGANIZATION		8b. OFFICE SYMBOL (If applicable)	9. PROCUREMENT INSTRUMENT IDENTIFICATION NUMBER			
8c. ADDRESS (City, State and ZIP Code)			10. SOURCE OF FUNDING NOS.			
			PROGRAM ELEMENT NO.	PROJECT NO.	TASK NO.	WORK UNIT NO.
11. TITLE (Include Security Classification) Thrust Generation by An Airfoil in Hovering Mode (U)			61102F		2307-F1	38
12. PERSONAL AUTHOR(S) Peter Freymuth						
13a. TYPE OF REPORT Research		13b. TIME COVERED FROM _____ TO _____		14. DATE OF REPORT (Yr., Mo., Day) 23 Jan 89		15. PAGE COUNT 31
16. SUPPLEMENTARY NOTATION						
17. COSATI CODES			18. SUBJECT TERMS (Continue on reverse if necessary and identify by block number) Unsteady Aerodynamics; Separated Flows; Dynamic Stall.			
FIELD	GROUP	SUB. GR.				
0101						
2004						
19. ABSTRACT (Continue on reverse if necessary and identify by block number) An airfoil is operated in combined plunging and pitching motion to generate a thrusting jet in a still air environment. The device serves as a simple, generic and two-dimensional model for hovering flight of small birds and insects. When properly tuned the device produces very large average thrust coefficients. The vortical signature of the tuned jet is a vortex street with reverse sense of rotation as the vortices of a Karman street.						
20. DISTRIBUTION/AVAILABILITY OF ABSTRACT UNCLASSIFIED/UNLIMITED <input checked="" type="checkbox"/> SAME AS RPT. <input type="checkbox"/> DTIC USERS <input type="checkbox"/>				21. ABSTRACT SECURITY CLASSIFICATION UNCLASSIFIED		
22a. NAME OF RESPONSIBLE INDIVIDUAL Peter Freymuth				22b. TELEPHONE NUMBER (Include Area Code) 719-472-3122		22c. OFFICE SYMBOL FJSRL/NHM

Thrust Generation by an Airfoil in Hovering Mode.

P. Freymuth. Visiting Professor at F. J. Seiler Research Laboratory,
USAF Academy, Colorado Springs.

(On sabbatical leave from University of Colorado, Boulder.)

Abstract

An airfoil is operated in combined plunging and pitching motion to generate a thrusting jet in a still air environment. The device serves as a simple, generic and two-dimensional model for hovering flight of small birds and insects. When properly tuned the device produces very large average thrust coefficients. The vortical signature of the tuned jet is a vortex street with reverse sense of rotation as the vortices of a Karman street.

Introduction

We found previously ^{1,2} that an airfoil which is exposed to a steady wind and which executes pure plunging or pure pitching motions can generate thrust similar to a flapping bird wing or a pitching fish tail. The vortical signature of this thrust generation is a vortex street with vortex rotation reverse to a Karman street, i.e., a two-dimensional jet. To obtain this thrust signature in a still air

for	<input type="checkbox"/>
1	<input checked="" type="checkbox"/>
2	<input type="checkbox"/>
3	<input type="checkbox"/>
4	<input type="checkbox"/>
5	<input type="checkbox"/>
6	<input type="checkbox"/>
7	<input type="checkbox"/>
8	<input type="checkbox"/>
9	<input type="checkbox"/>
10	<input type="checkbox"/>

11	<input type="checkbox"/>
12	<input type="checkbox"/>
13	<input type="checkbox"/>
14	<input type="checkbox"/>
15	<input type="checkbox"/>
16	<input type="checkbox"/>
17	<input type="checkbox"/>
18	<input type="checkbox"/>
19	<input type="checkbox"/>
20	<input type="checkbox"/>
21	<input type="checkbox"/>
22	<input type="checkbox"/>
23	<input type="checkbox"/>
24	<input type="checkbox"/>
25	<input type="checkbox"/>
26	<input type="checkbox"/>
27	<input type="checkbox"/>
28	<input type="checkbox"/>
29	<input type="checkbox"/>
30	<input type="checkbox"/>
31	<input type="checkbox"/>
32	<input type="checkbox"/>
33	<input type="checkbox"/>
34	<input type="checkbox"/>
35	<input type="checkbox"/>
36	<input type="checkbox"/>
37	<input type="checkbox"/>
38	<input type="checkbox"/>
39	<input type="checkbox"/>
40	<input type="checkbox"/>
41	<input type="checkbox"/>
42	<input type="checkbox"/>
43	<input type="checkbox"/>
44	<input type="checkbox"/>
45	<input type="checkbox"/>
46	<input type="checkbox"/>
47	<input type="checkbox"/>
48	<input type="checkbox"/>
49	<input type="checkbox"/>
50	<input type="checkbox"/>



A-1

environment, i.e., during hovering flight, it has been stated ¹ that a combination of plunge and pitch motions of the airfoil would be needed. In this paper we follow up on this concept by designing and investigating a thin airfoil which executes the appropriate periodic plunge-pitch motions in a still air environment.

Our apparatus is intended as a basic, two-dimensional generic model of the unsteady hovering flight of small birds and insects. In contrast, the mainstream literature ³⁻⁹ is very animal specific (humming birds, dragon flies, chalcid wasps, etc.), and therefore, very complex and hard to interpret from an aerodynamic point of view. It is hoped that these simple and complex approaches are synergistic.

Dimensional considerations and modes of hovering.

Consider a thin, flat plate airfoil with chord length c exposed to still air and executing a translating (plunging) motion h in horizontal direction:

$$h = h_a \sin 2 \pi f t \quad (1)$$

where h_a is the amplitude of translation, f is the frequency of oscillation and t is time. Consider the airfoil to simultaneously execute a pitching motion around the half-chord axis:

$$\alpha = \alpha_o + \alpha_a \sin(2 \pi f t + \phi) \quad (2)$$

where α is the angle of attack with respect to the horizontal line, α_o is the average angle of attack, α_a is the pitch amplitude and ϕ is the phase difference between pitching and plunging. Our experimental apparatus is designed to allow within some limits combined plunging-pitching motions of the airfoil.

Appropriate dimensionless parameters of the system are: α_o, α_a, ϕ , the dimensionless plunge amplitude h_a/c and a Reynolds number $R_f = 2\pi f h_a c / \nu$ based on maximum plunge speed and on c , where ν is the kinematic viscosity.

The simplest modes of hovering identified and solely investigated in this paper are: Mode 1 or "water treading mode" characterized by $\alpha_o = 0$ and $\phi = \pi/2$ (90°), as sketched in Fig. 1. In this mode leading and trailing edges switch their role during one cycle of oscillation. The resulting hover-jet as sketched is thrown upward, with thrust on the airfoil pointing downward. Since the apparatus is mounted on the ground and obstructs the view in downward direction, we intentionally let the jet develop in upward direction, in contrast to insect hovering. The other mode investigated is mode 2 or "degenerate figure eight mode" characterized by $\alpha_o = \pi/2$ (90°) and $\phi = -\pi/2$ (-90°). As sketched in Fig. 2, in this mode leading and trailing edges do not switch their role during one cycle.

Thrust coefficient of the hover-jet.

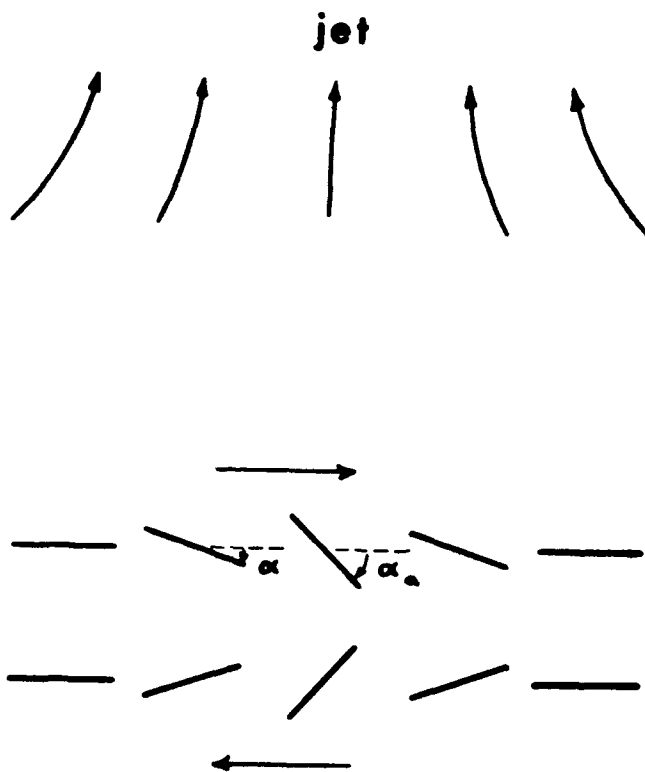


Fig. 1 Sketch of combined translating-pitching motion of the airfoil during one cycle for mode 1 hovering.

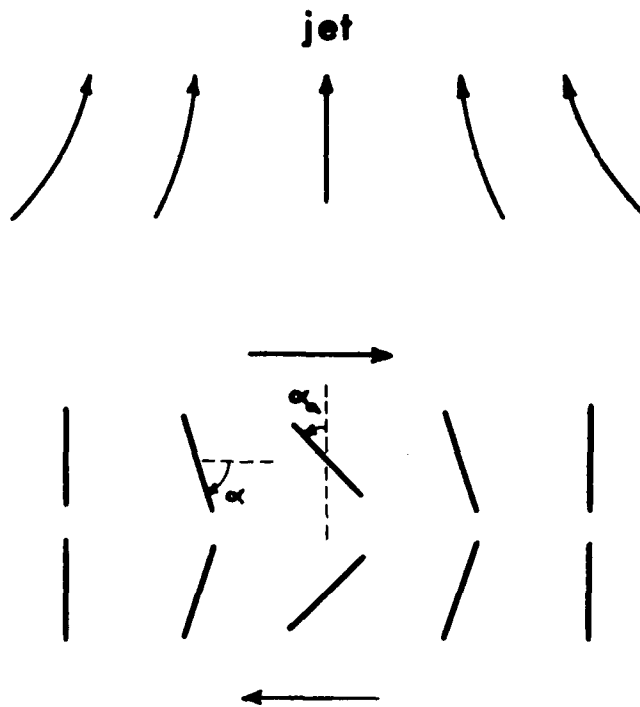


Fig. 2 Sketch of combined translating-pitching motion of the airfoil during one cycle for mode 2 hovering.

Detailed experimental results on the hover-jet will be shown later on. Our concept of such a jet is best illustrated at this point by a flow visualization example in Fig. 3. The hovering airfoil near the bottom of the figure generates a vortex street which is marked by smoke. The left column of vortices is staggered compared to the right column and these vortices induce on each other an upward motion. This upward moving somewhat turbulent hover jet generates thrust on the airfoil in downward direction.

To characterize the time averaged thrust T on the airfoil, let us define a thrust coefficient C_T :

$$C_T = \frac{T}{\frac{\rho}{2} \overline{V_t^2} c \cdot \ell} \quad (3)$$

where ρ is the air density, $\overline{V_t^2}$ is the mean square speed of the horizontal airfoil motion and $\ell \gg c$ is the span of the airfoil. From the kinematics of the translating motion

$$\overline{V_t^2} = 0.5 (2\pi f h_a)^2 \quad (4)$$

and from the momentum theorem

$$T = \rho \ell \int_{-\infty}^{\infty} \overline{V^2} dx \quad (5)$$

where $\overline{V^2}$ is the mean square velocity in the jet at a sufficient distance above the airfoil where the jet has acquired ambient



Fig. 3 Single photograph of a hover-jet for mode 1 hovering of the airfoil. $h_a = 2.54\text{cm}$, $\alpha_a = 68^\circ$, $f = 1\text{ Hz}$, $h_a/c = 1$, $R_f = 230$.

pressure, x is the horizontal coordinate across the jet. The thrust coefficient of the jet therefore is:

$$C_T = \frac{\int_{-\infty}^{\infty} \overline{V^2} dx}{(\pi f h_a)^2 c} \quad (6)$$

Thrusting would of course be upward during actual hovering and the jet directed downward. The thrust coefficient C_T may therefore also be considered a lift coefficient of the hovering airfoil.

The purpose of our paper will be the experimental determination of C_T over a limited parameter range and the visualization of the vortical signatures of the hover-jet.

Experimental apparatus and procedures.

The experiment allows a small airfoil to execute combined plunging and pitching motions and is sketched in Fig. 4. The planar airfoil has a thickness of 1.6 mm with rounded edges, a chord $c = 2.54$ cm and a span $b = 30.5$ cm. The airfoil is mounted on a slide frame which is driven in nearly sinusoidal horizontal translation by means of a dc-motor which is mounted on the fixed main frame of the apparatus. The motor rotates the drive wheel which connects to the slide frame by means of a drive rod as shown. In order to generate the simultaneous pitching motion for the airfoil a "slave wheel" is mounted on the slide frame and connects via another drive rod to the

fixed main frame. This arrangement forces the slave wheel to execute the same rotation as the drive wheel. The drive rods are elastically anchored to avoid jamming of the drive mechanism. The axis of the slave wheel also carries the pitch wheel which connects via the pitch rod to the pitch lever of the airfoil.

The pitch wheel can be rotated against the slave wheel and the amount of preset rotation determines the phase angle (in our experiments $\phi = \pm 90^\circ$). The airfoil chord can be rotated against the lever and this way α_o can be adjusted (0° in mode 1, 90° in mode 2). The pitch amplitude α_a can be adjusted to values 25° , 33° , 42° , 50° and 68° by inserting the drive rod axis into holes of different radial distance on the pitch wheel. The plunge amplitude h_a can be adjusted to values 1.54 cm, 3.81 cm, 5.08 cm and 6.35 cm by linking both drive rods to holes at these radial distances in the drive and slave wheels. The rotation rate f of the dc-motor can be regulated between 1 and 6 Hz and was measured by means of a reed switch connected to an electronic counter.

A photograph of the apparatus is shown in Fig. 5 for additional orientation. This photo also shows the Pitot tube above the apparatus which was used in connection with a sensitive pressure transducer to determine the dynamic pressure profile across the jet. This allows, according to eq. 6, the determination of C_T . The pressure transducer was connected to a digital voltmeter with a time constant of 20 sec. for averaging purpose.

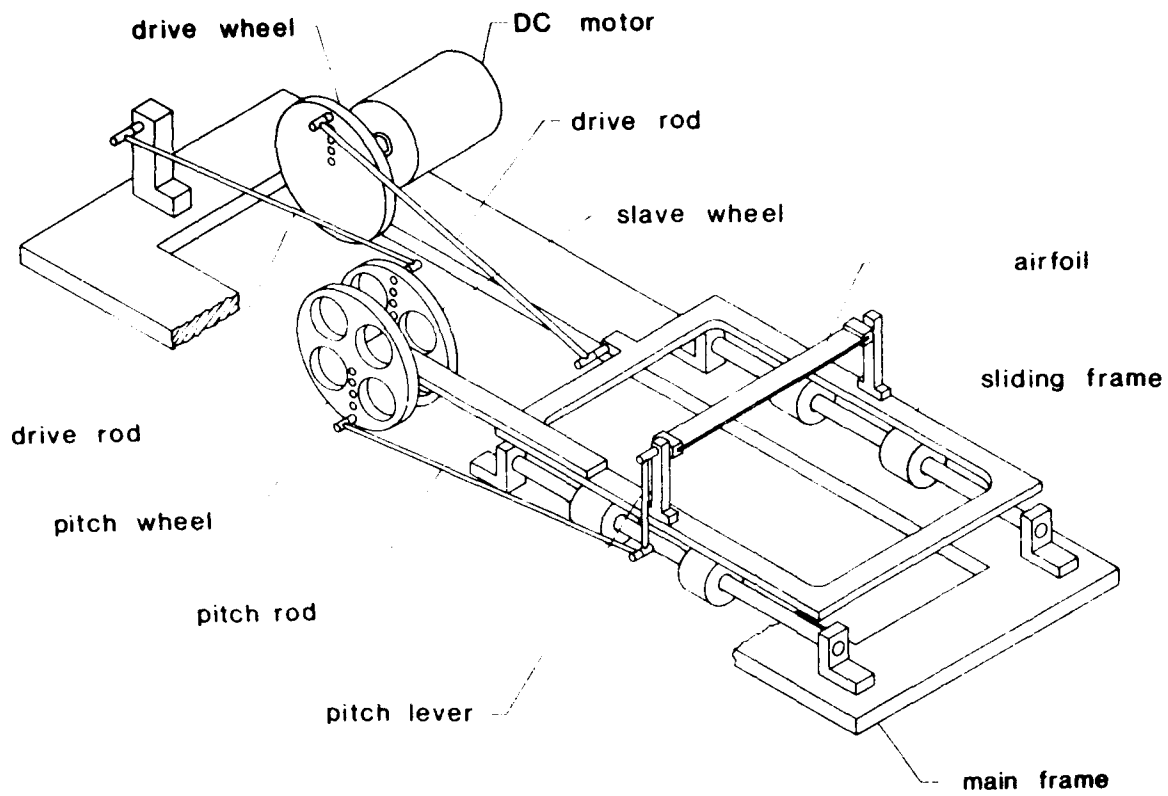


Fig. 4 Sketch of experimental apparatus.

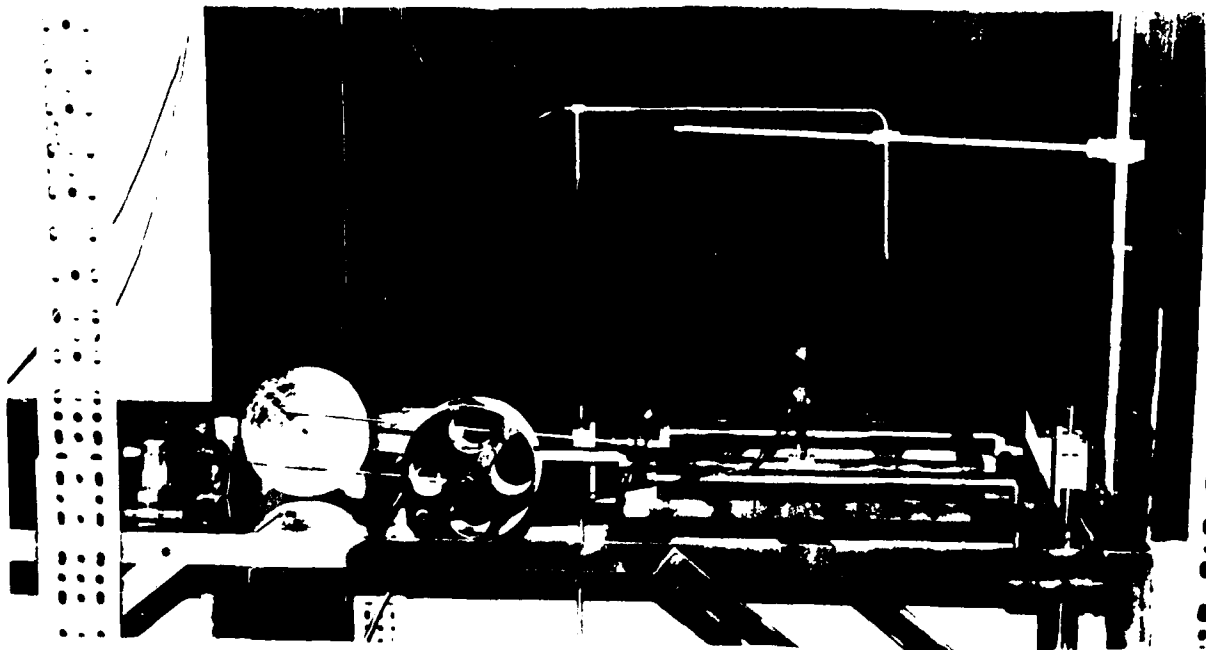


Fig. 5 Photograph of experimental apparatus.

Flow visualization is by means of the titanium-tetrachloride method of vortex tagging¹⁰. A liquid film of $TiCl_4$ is deposited on the airfoil as a center strip using a brass pipette. The white fumes which develop tag the vorticity generated in the boundary layer of the airfoil and make separation and subsequent vortex developments visible, when photographed in side view. The airfoil was floodlit from above as well as below. Movies were taken with a Bolex 16mm movie camera at a rate of 64 frames/sec.

Experimental results.

Velocities in the hover-jet were of order 1m/sec at best taxing somewhat the use of the Pitot tube for velocity profile determination. Most measurements of C_T were conducted at the highest Reynolds number our apparatus allowed, i.e., $R_f = 1700$. Dependence of airfoil forces on Reynolds number is usually weak¹¹. Velocity profiles were measured 8 chord lengths above the airfoil and a typical example is shown in Fig. 6. Squaring these profiles and graphic integration yields thrust coefficients C_T according to eq. 6. In this way C_T was determined for the limited parameter range of h_a/c and α_a available to us both for mode 1 and mode 2 operation of the airfoil. Fig. 7 summarizes the results obtained in mode 1 operation and Fig. 8 those in mode 2 operation. The most outstanding features of these results are the extraordinarily high thrust coefficients which can be reached, up to at least 12 in mode 1 and 7.4 in mode 2. If correct, thrust coefficients of 6 reported for dragonflies by Norberg⁵ would not seem out of line. Independent

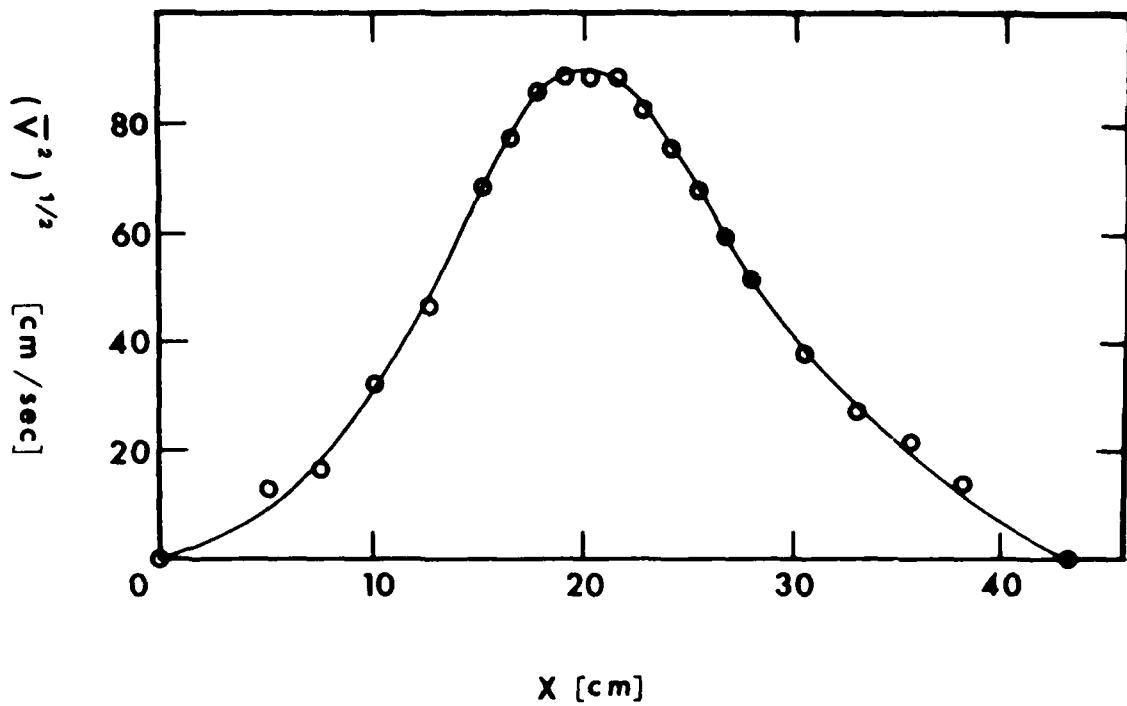


Fig. 6 Example of a velocity profile of the hover-jet measured with Pitot tube 8 chord lengths above the airfoil.
 $h_a = 3.81\text{cm}$, $\alpha_a = 68^\circ$, $f = 5\text{Hz}$, mode I hovering.

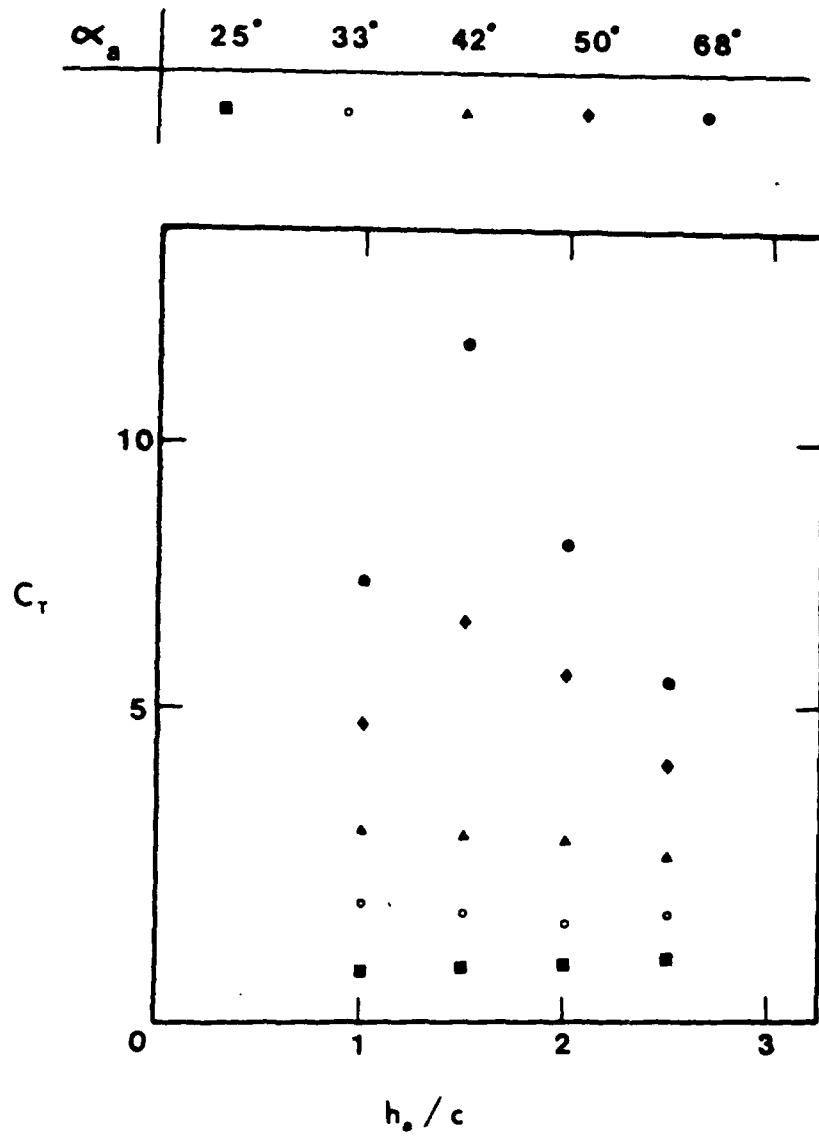


Fig. 7 Thrust coefficient C_T versus h_a/c and α_a for mode 1 hovering.

α_a	25°	33°	42°	50°
	•	♦	▲	■

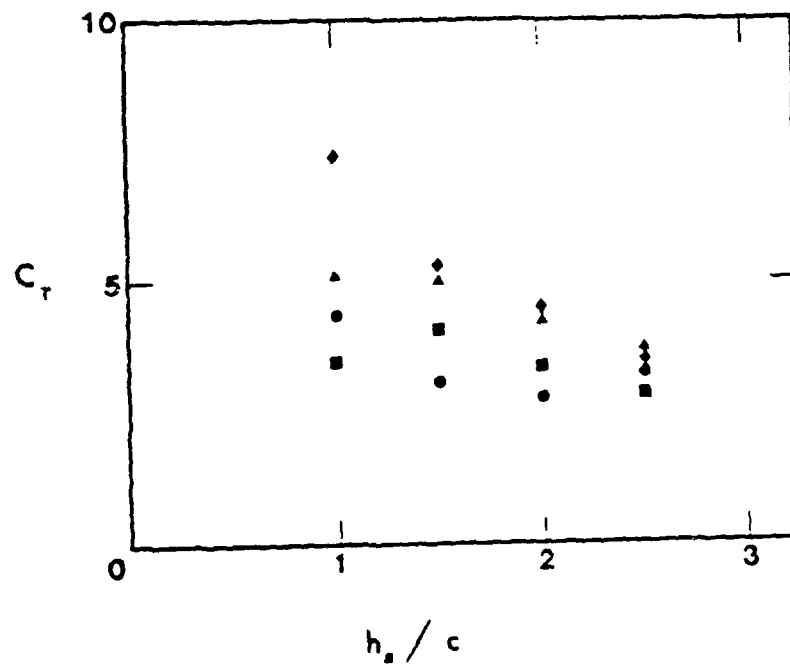


Fig. 8 Thrust coefficient C_T versus h_a/c and α_a for mode 2 hovering.

Note: Results of Figs. 7-8 are preliminary only.

confirmation of high thrust coefficients found by us seems however to be an urgent need.

It has been thought that large thrust coefficients found for some insects could only be the result of special interactions of a pair of wings, like proper phasing in dragonfly wing beats^{8,9} or the clasp and fling mechanism for the chalcid wasp.^{3,4,6} It came as a surprise that high thrust coefficients could be reached by our generic hovering experiments with a single airfoil. According to Figs. 7 and 8 all that is required for large thrust coefficients are fairly small plunge amplitudes of order of a chord length and angles of attack of order of 60° reached at some point in the cycle. In other words "tuning" of the hovering airfoil for high thrust coefficients is quite simple.

Figs. 9 and 10 show single photographs of well tuned hover-jets in mode 1 and mode 2 operations. Both cases show almost identical vortex features, i.e., alternate vortices forming a simple vortex street indicative of a jet. In contrast, Fig. 11 shows a hover-jet "out of tune," i.e., far from maximum thrust coefficient. In this case a complex and pretty vortex tapestry¹² develops which should however be quite inefficient in creating a highly directed jet.

Fig. 12 shows a sequence of an entire cycle of airfoil oscillation, in mode 1 operation with $\alpha_a = 68^\circ$ and $h_a/c = 1.5$, for which a large C_T is obtained. Frames are ordered into columns from top to bottom, columns are ordered from left to right. Time between consecutive



Fig. 9 Single photograph of well-tuned mode 1 hover-jet.
 $h_{jet} = 1.5$, $\alpha_a = 68^\circ$, $f = 1$ Hz. $Re = 340$.



Fig. 10 Single photograph of well-tuned mode 2 hover-jet.
 $h_a/c = 1$, $\alpha_a = 33^\circ$, $f = 1.3$ Hz, $R_f = 300$.



Fig. 11 Single photograph of mode 1 hover-jet far from optimum thrust. $h_a/c = 1.5$, $\alpha_a = 25^\circ$, $f = 1$ Hz, $R_f = 340$.

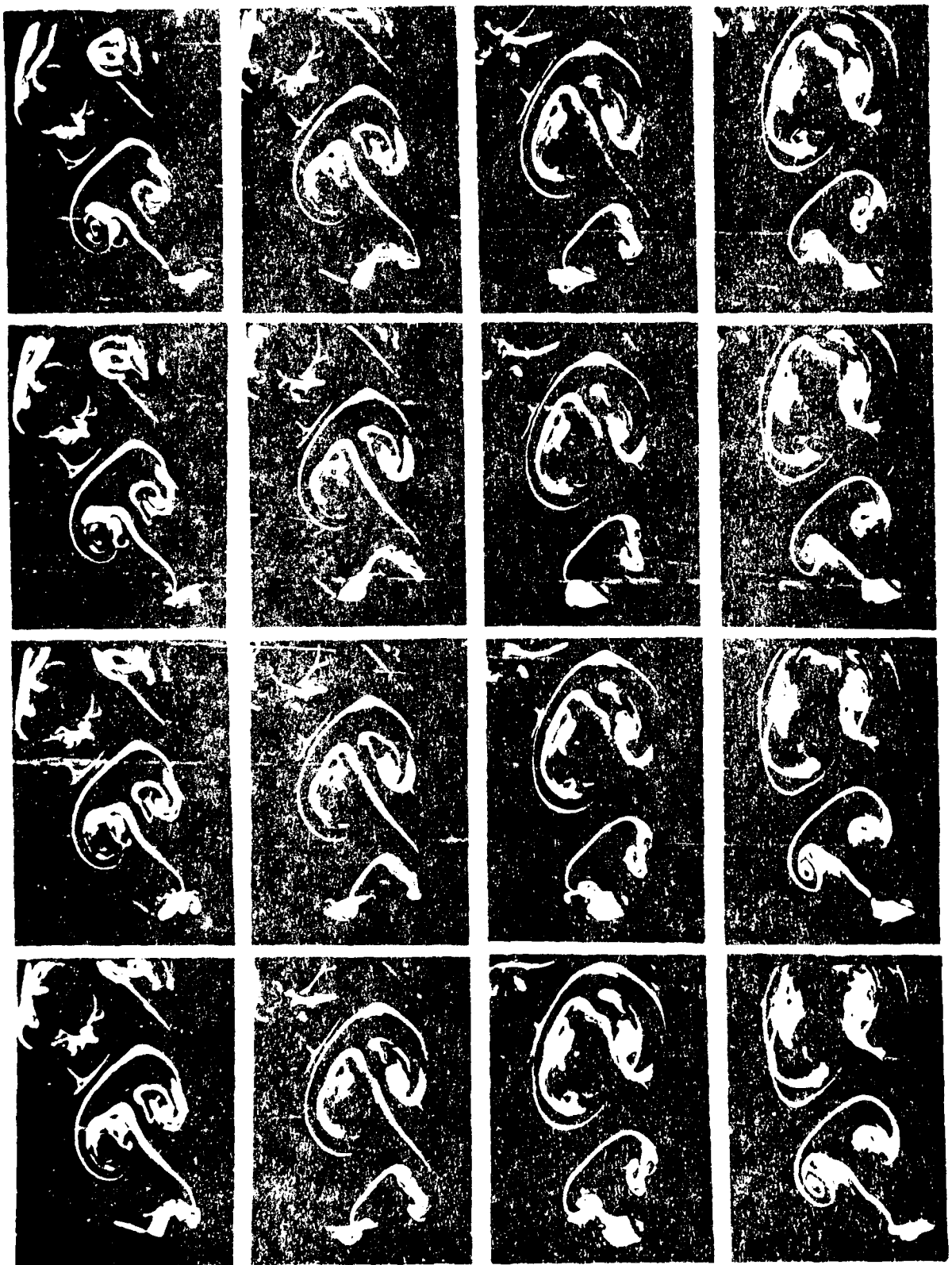


Fig. 12 Sequence of mode 1 hover-jet. $h_a/c = 1.5$, $\alpha_a = 68^\circ$.

$f = 1$ Hz. $R_f = 340$, $\Delta t = 1/16$ sec.

frames is $\Delta t = 1/16$ sec. Frame 1 shows the airfoil in its farthest right position. From there to the bottom of column 2 the airfoil moves to its farthest left position and in the process creates a clockwise rotating vortex. The last 2 columns show the airfoil moving to the right again creating in the process a counterclockwise rotating vortex to the left and below the previously generated clockwise vortex. This process repeats during each cycle and the result is a vortex street or hover-jet.

The vortex generation near the airfoil is quite complicated as a closeup sequence, taken slightly from the left, reveals in Fig. 13. In this case the first frame shows the airfoil passing through the $h=0$ position from left to right, where the airfoil reaches its maximum angle of attack. This way we focus on the development of the dynamic stall vortex in the first column. In the second column this vortex partly rolls over the left edge of the airfoil and gets severed during the leftward motion of the airfoil in column 2. The severed parts of the vortex then amalgamate with the vorticity which is generated and shed from the right edge of the airfoil and form a single clockwise vortex by the end of column 2. An analogous process creates the counterclockwise vortex but would need observation slightly from the right.

The process of vortex severing is shown even more pristinely in Fig. 14 which represents only part of a sequence but at a time resolution $\Delta t = 1/64$ sec. Vortex severing has been previously discovered by Ziada and Rockwell¹³ in a different context.

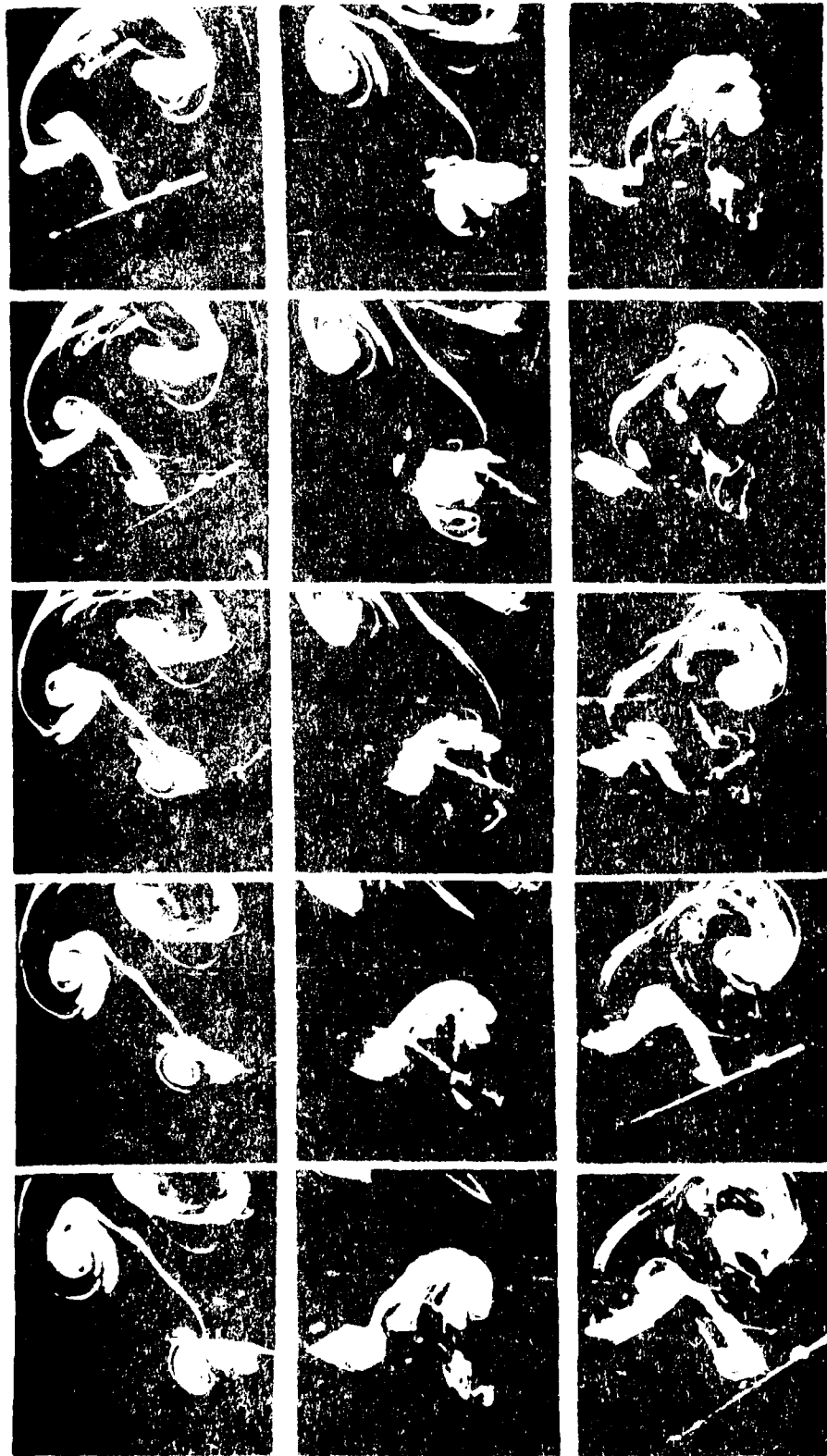


Fig. 13 Closeup sequence of mode 1 hover-jet.

$h_a/c = 1.5$, $\alpha_a = 63^\circ$, $f = 1.2$ Hz, $R_f = 400$, $\Delta t = 1/16$ sec.



Fig. 14 Part of a closeup sequence of mode 1 hover-jet with increased time resolution. $b_j = 1.5$, $R_j = 340$, $f = 1$ Hz, $R_f = 340$, $\Delta t = 1/64$ sec.

Amalgamation of vortices of the same sense of rotation but without prior severing were also observed if the airfoil was operated in mode 2 and tuned for high thrust coefficients. A sequence is shown in Fig. 15. It should be mentioned that because of the limited parameter range of h_a/c and α_a available to us the question what the absolute maxima of C_T in modes 1 and 2 will be remains open.

It should be mentioned that flow visualizations shown are at fairly low Reynolds numbers where flow visualization is mostly laminar. At the higher Reynolds numbers where thrust coefficients were measured, the hover-jet assumes a more turbulent appearance characterized by diffuseness of smoke visualization. Nevertheless, basic large scale features seem to be the same as at lower Reynolds numbers. The sequences of tuned mode 1 and mode 2 jets shown in Figs. 16 and 17 may serve to support this statement.

Conclusion and outlook.

It has been shown that an airfoil executing appropriate combined plunging and pitching motions can acquire very large thrust coefficients in a still air environment. There exists an urgent need for independent corroboration of these results. An extension of the parameter range to be investigated would also be helpful. The vortical signature of high thrust is a simple vortex street with the character of a jet stream. It is hoped that the experiments reported here will also advance the understanding of the more complex

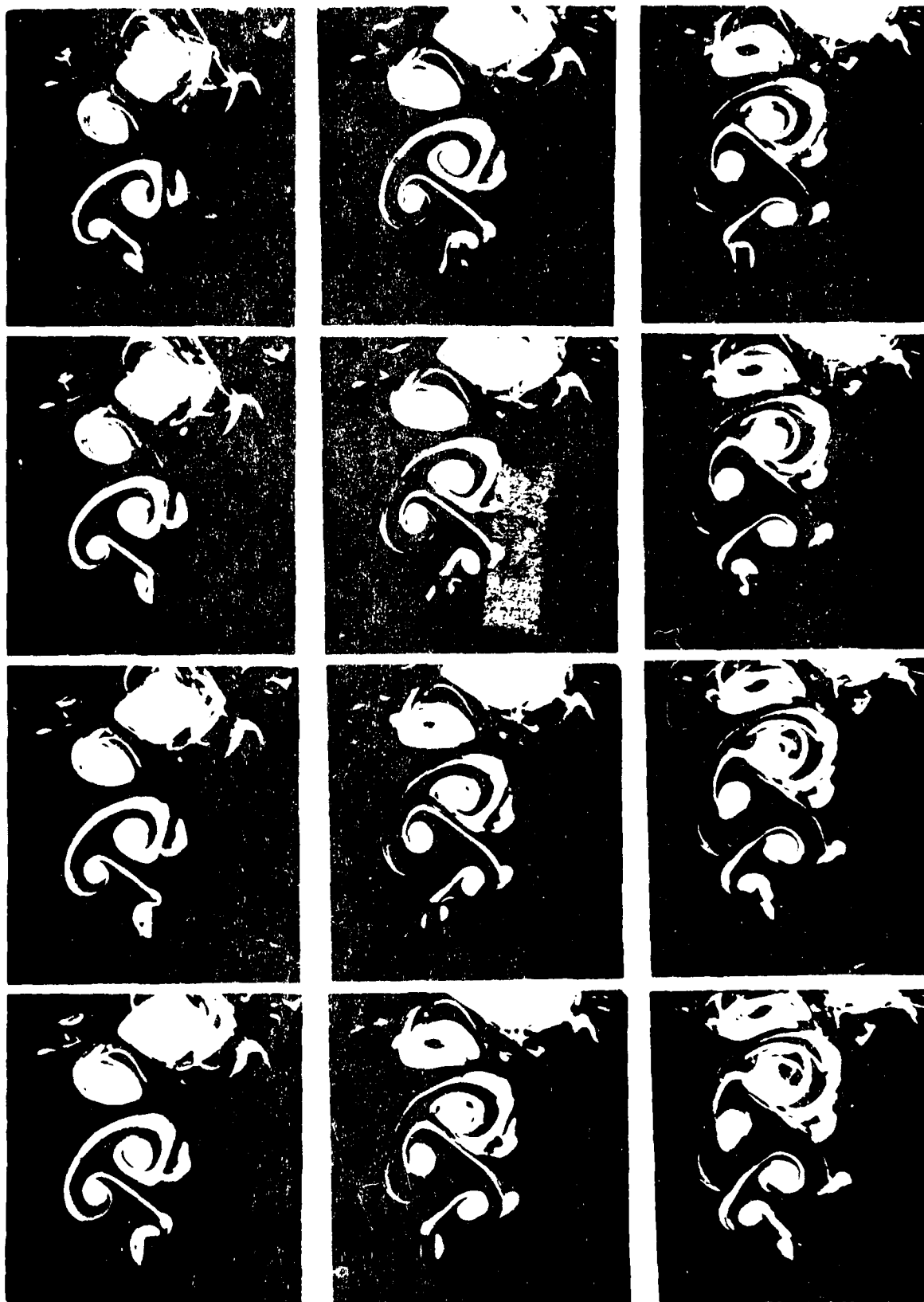


Fig. 15. Sequence of mode 2 (reverberant)

Time = 1.547 sec. $f_c = 13.47$ Hz. $B_0 = 300$ Hz. $\Delta t = 1/16$ sec.

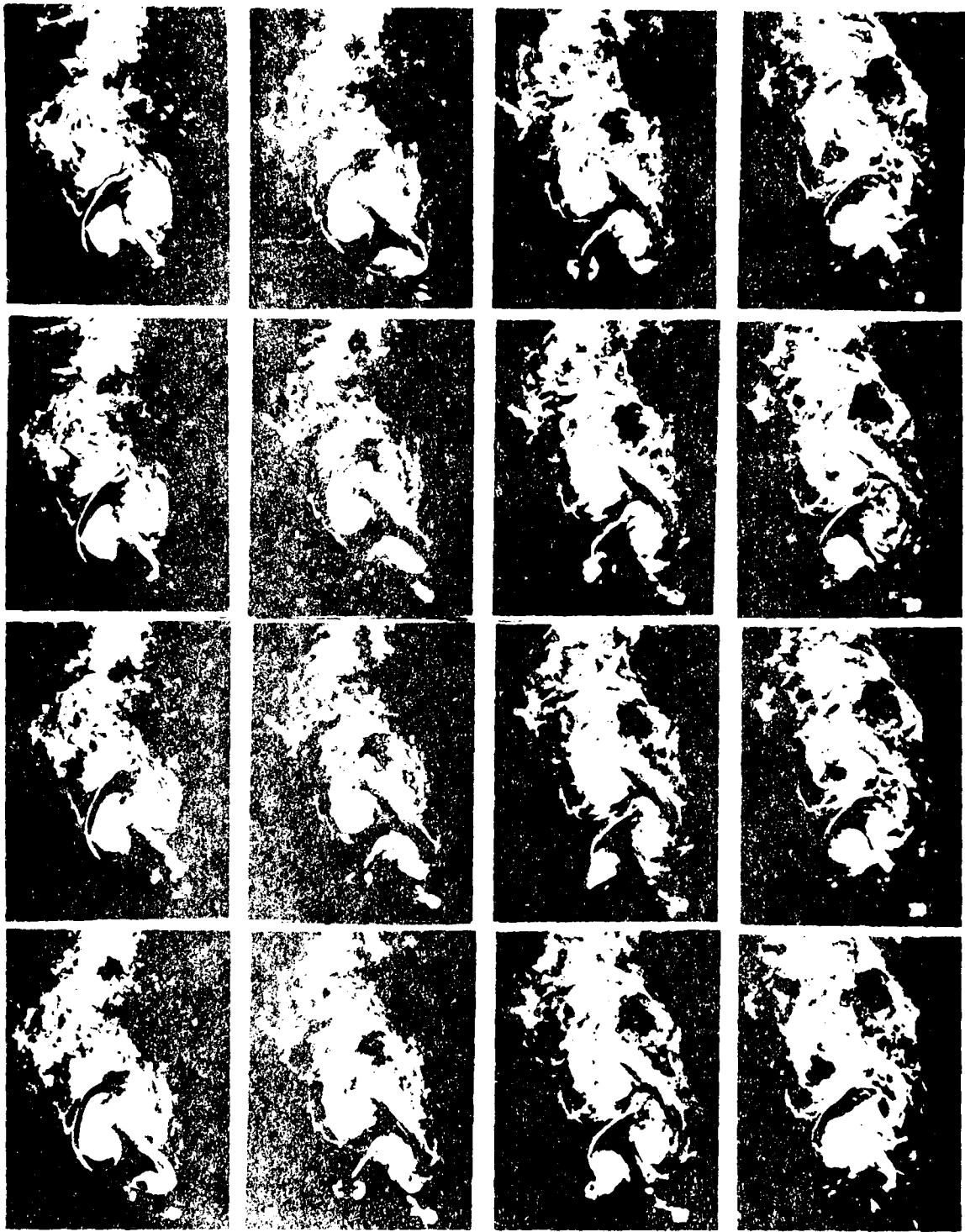


Fig. 16 Sequence of mode 1 hover-jet at higher Reynolds number.

$h_0/c = 1.5$, $\beta_a = 68^\circ$, $f = 4$ Hz, $R_f = 1400$, $\Delta t = 1/64$ sec.

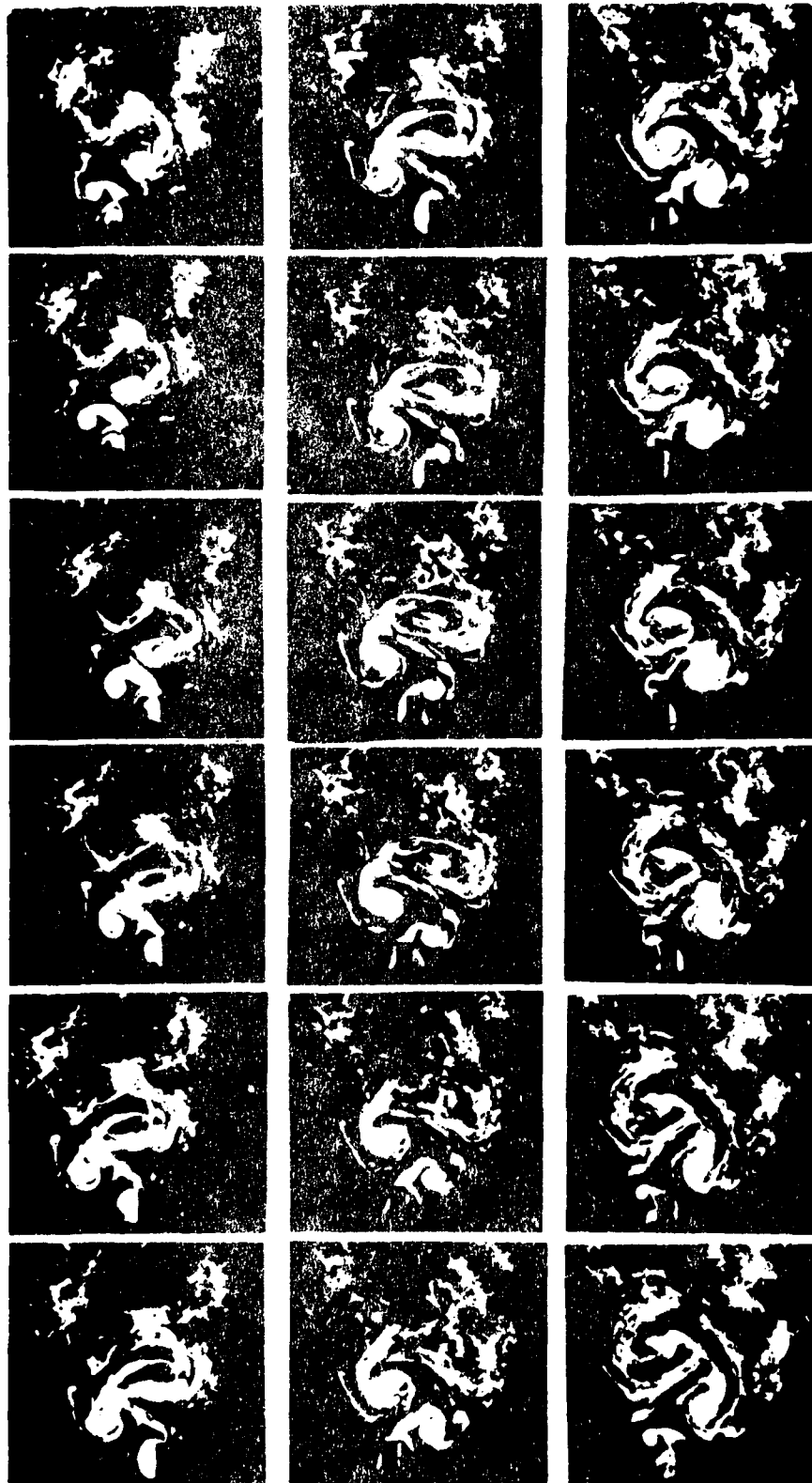


Fig. 17 Sequence of mode 2 hover-jet at higher Reynolds number.

$h_a/c = 1$, $\alpha_a = 33^\circ$, $f = 4$ Hz, $R_f = 900$, $\Delta t = 1/64$ sec.

hovering flight of small birds and insects. Since the model is two-dimensional, computer modelling is a distinct possibility to further advance understanding.

Acknowledgements

The author acknowledges a visiting professorship at the F. J. Seiler Research Laboratory, sponsored by the Air Force Systems Command. An AFOSR Grant F49620-84-C-0065, H. Helin program manager, provided additional assistance. The author is indebted to M. Luttges, M. Robinson, R. Reilman, and J. Walker for helpful discussions. Photocredit goes to W. Bank, the experimental apparatus was built by R. Hatfield and illustrations were provided by R. Tarasewicz.

References

1. Freymuth, P., Propulsive vortical signature of plunging and pitching airfoils. Paper AIAA-88-0323, 1988.
2. Freymuth, P. Propulsive vortical signature of plunging and pitching airfoils. AIAA. J. Vol. 26, pp. 881-883, 1988.
3. Lighthill, J. Aerodynamic aspects of animal flight. In "Swimming and Flying in Nature," Wu, Y., Brokaw, C., Brennen, C. (eds.), Vol II, pp. 423-491, Plenum Press, New York, 1975.
4. Weis-Fogh, T. Flapping flight and power in birds and insects, conventional and novel mechanisms. In "Swimming and Flying in Nature," Wu, Y., Brokaw, C., Brennen, C. (eds.), Vol. II, pp. 729-762, Plenum Press, New York, 1975.
5. Norberg, R. A. Hovering flight of the dragonfly *Aeschna Juncea* L., kinematics and aerodynamics. In "Swimming and Flying in Nature," Wu, Y., Brokaw, C., Brennen, C. (eds.), Vol. II, pp. 763-81, Plenum Press, New York, 1975.
6. Maxworthy, T. The fluid dynamics of insect flight. Ann. Rev Fluid Mech., Vol. 13, pp. 329-350, 1981.
7. Soms, C., Luttges, M., Dragon flight: Novel uses of unsteady separated flows. Science, Vol. 228, pp. 1326-1329, 1985.

8. Reavis, M. A., Luttgies, M. W. Aerodynamic forces produced by a dragonfly. Paper AIAA-88-0330, 1988.
9. Saharon, D., Luttgies, M. W., Dragonfly unsteady aerodynamics: The role of the wing phase relations in controlling the produced flows. Paper AIAA-89-0832, 1989.
10. Freymuth, P., Bank, W., Palmer, M. Use of titanium tetrachloride for visualization of accelerating flow around airfoils. Flow Visualization III, Hemisphere Publishing Corp., pp. 99-105, 1985.
11. Robinson, M.C., Wissler, J.B. Pitch rate and Reynolds number effects on a pitching rectangular wing. Paper AIAA 88-2577-CP, 1988.
12. Freymuth, P. Vortices, Handbook of Flow Visualization, W.-J. Yang, editor, Hemisphere Publishing Corp., pp. 459-479, 1989.
13. Ziada, S., Rockwell, D. Vortex-leading edge interaction. J. Fluid Mech., Vol. 118, pp. 79-107, 1982.